



CAD Based Geometric and Force Modeling of Single Point Form-cutting Tools

K Sambhav¹, P Tandon² and S G Dhande³

¹Indian Institute of Technology, Kanpur, India, sambhav@iitk.ac.in

²PDPM Indian Institute of Information Technology, Jabalpur, India, ptandon@iiitdmj.ac.in

³Indian Institute of Technology, Kanpur, India, sgd@iitk.ac.in

ABSTRACT

The paper models Single Point Cutting Tools (SPCTs) with free-form rake and flank surfaces for geometry and cutting forces using CAD. The geometric profile of the rake and flank surfaces has been modeled using NURBS where the control points can be arbitrarily chosen and interactively modified to obtain the desired cutting angles along the cutting edge. Such a model can be employed to design form-cutting tools with optimum profile. The geometric model is used to calculate the rake and flank angles in the prevalent nomenclatures such as ASA, ORS and NRS by obtaining projections to the normal along the cutting edge on the chosen planes. The angles are then used to predict the cutting and thrust forces using a mechanistic equation for HSS tool and MS work-material combination. To validate the results, an HSS tool is ground arbitrarily and the points on the cutting edge and rake face are captured. The control points are derived and the model is fitted to generate the geometry of the tool. Experiments are conducted for different machining conditions and the theoretical and experimental results are compared. The results show a good correlation with the prediction.

Keywords: single point cutting tool, free-form, NURBS, mechanistic model.

DOI:10.3722/cadaps.2013.45-57

1 INTRODUCTION

The recent developments in the aeronautic and automobile industries have necessitated high production of sculptured geometries. The machining of sculptured surfaces requires design of form-cutting tools for efficient and error free manufacturing. The geometry of the surface machined is a direct function of the geometry of the cutting tool surfaces along with the relative motion between them. This is based on the fact that the surface of the cutter in contact with the workpiece and the machined surface are mutually enveloping surfaces [1]. The sculptured cutting edges and surfaces of form-cutting tools employed for sculptured surface machining (SSM) can be suitably modeled using CAD. A CAD definition of the cutting tool is able to model the face and flanks of the tool with

arbitrarily chosen data points along the edges and surfaces. Such a definition is sufficient to generate the point cloud data for the surface model of the tool. The definition of the surfaces can be given in terms of any of a composite Ferguson, Bezier, B-spline or NURBS surface depending on the requirement. NURBS surfaces give a local control of the shapes and are more useful for the purpose. These definitions can then be used for calculation of angles on the tool. Or, if the tool angles are provided, the surfaces can be interactively altered and required surfaces can be generated. The geometric modeling has to be followed by force modeling so that the cutting forces, tool wear, tool life, etc. can be predicted.

Machining of sculptured surfaces using 3-axis and 5-axis CNC machines has gained interest in many academic circles in the past decade. Radzevich [2] has worked extensively on SSM and presented the approach of R-mapping of a sculptured surface on to the machining surface of a form cutting tool assuming one to one correspondence between their principal curvatures. He presented a set of six necessary and sufficient conditions for proper sculptured surface machining [3]. In his another work [4], the method to design a form-cutting tool for optimum machining of a sculptured surface on a multi-axis NC machine has been proposed. Many authors have presented the tool path or orientation judgment strategy while machining a sculptured surface on a multi-axis CNC machine to avoid the problems of cutter gouging, inadequate tool accessibility, poor surface finish, cusp height errors etc. To name a few, Fan and Ball [5] have presented a quadric method for cutter orientation in five-axis sculptured surface machining to maximize the machining efficiency at a cutter contact point. Li and Jerard [6], and Lee [7] have given algorithms to generate gouge-free, non-isoparametric 5-axis tool paths. Fussel et al. [8] have simulated SSM on a 5-axis CNC using two different geometric models for the tool and the workpiece. Liu [9] has used the basic concepts of differential and analytical geometry to present an algorithm for the toolpath generation of five-axis cylindrical milling of sculptured surfaces with cylindrical cutter. Park [10] has presented two algorithms to optimize the procedure for tool path generation in regional milling using triangular mesh slicing. Zhongqing [11] has brought out the shortcomings of a 2D representation of a cutter and modeled a 3D cutter using vector representation and presented the model of a turning cutter as an example. Sambhav et al. [12] have presented a generic mathematical model of the geometry of a single point cutting tool in terms of grinding parameters.

A survey of the force modeling for SSM shows that mechanistic modeling has proven to be a strong tool as its semi-empirical approach uses the benefits of both the analytical and empirical methods and proposes a realistic force model for curved surfaces. Lamikiz et al. [13] estimated the cutting forces in up-milling and down-milling of inclined surfaces based on a semi-mechanistic model taking the material, the tool, the cutting conditions, the machining direction and the slope of the surface as variables. Lazoglu [14] has given a generalized mechanistic model of ball-end milling force system for SSM capable of calculating the workpiece/cutter intersection for a given cutter location and geometry. Fussel et al. [8] have employed the geometric models to calculate the tool contact area used to calculate the cutting forces mechanistically. Sambhav et al. [15] have used the generic geometric model [12] to generate a regression model for the cutting forces by a single point cutting tool in terms of the tool grinding angles.

The presented work employs the mechanistic equations given by [15] to evaluate the cutting forces of form-tools using NURBS as the basic tool for geometric modeling. This will help generate a generic model of such tools. The model starts with the assumption that the points on the cutting edge of the tool have been prudently derived using geometric conditions for proper conformity of the tool and

workpiece surfaces. The model is used to derive the tool angles and their representation in different nomenclatures. The angles are then used to predict the forces in cutting based on the comprehensive mechanistic model.

2 PREVALENT NOMENCLATURE AND SIGN CONVENTION FOR SPCT

SPCTs have been designated using different nomenclatures with the symbols used for tool signature in their standard order given below. The presented model will employ the same symbols throughout.

- 1) American Standards Association (ASA)

$$\gamma_z - \gamma_x - \alpha_z - \alpha_x - \phi_e - \phi_s - r$$

The auxiliary flank clearance angles are given by α'_z and α'_x .

- 2) Orthogonal Rake System (ORS)

$$\lambda - \gamma_o - \alpha_o - \alpha'_o - \phi_e - \phi - r$$

- 3) Normal Rake System (NRS)

$$\lambda - \gamma_n - \alpha_n - \alpha'_n - \phi_e - \phi - r$$

For a standard right hand turning tool, the angles are taken as positive if the tool rake face slopes away from the nose point. If the face slopes towards the nose in transverse or longitudinal direction, then that angle is regarded as negative. All the nomenclatures also follow the same convention. For the clearance angles, they are taken as positive when the gap between the tool flank and the work surface grows as one moves away from the tool tip. An acute principal cutting edge angle gives positive side cutting edge angle and vice-versa. The end cutting edge angle is treated as negative when it goes closer to the shank as the distance from the tool tip increases.

3 NURBS MODEL OF FORM-CUTTING TOOL

Before we model a form-cutting tool, we need to discuss the basic form of a cutting tool. Analysis shows that every standard metal cutting tool has the basic shape of a smooth symmetric wedge with flat faces and uniform depth (Fig. 1) having wedge angle as β , the incident force as P and the reaction as N . The proper selection of the inclination of the wedge faces with the work surface along different directions facilitates the smooth production of chips during cutting.

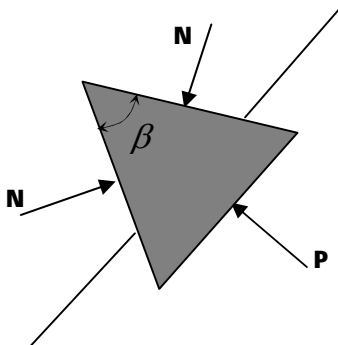


Fig. 1: A smooth symmetric wedge with flat faces.

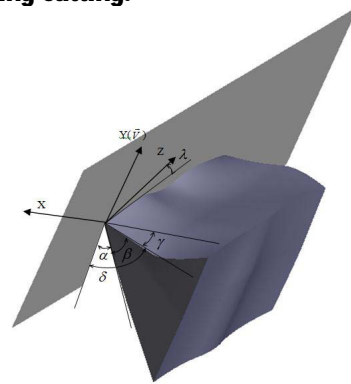


Fig. 2: Angles on the generic model of a tool.

When the tool is given a generic profile, the wedge is made up of free-form surfaces (Fig. 2) where the angles of orientation of the wedge surfaces with the work surface vary along the surface of the wedge giving the tool a very complex geometry and a difficult-to-perceive distribution of forces. The cutting angles have to be evaluated using tangents and normals at every point, and then the forces are calculated as a summation of the elemental force contributions of the discrete elements on the rake face along the cutting edge using analytical or semi-empirical or empirical methods. Here, the semi-empirical method is used. To employ this method, a correspondence between the prevalent nomenclatures and the generated profile is developed so that the prevalent understanding can be used to predict the behavior of the tool during cutting.

Every cutting tool has a wedge angle β , a cutting angle δ , a clearance angle α , a rake angle γ and an inclination angle λ associated with it. When δ is greater than $\pi/2$, γ is negative. A generic cutting tool has these angles varying from point to point as the cutting edges may be curved in space (Fig. 2). An effective geometric model of a generic SPCT will form the basis of modeling generic multi-point cutting tools. The application of such designs of tools can be found in the form of generic drill point geometry, an arbitrarily shaped mill, and form tools.

Before generating the definition of the cutting surfaces, a tool blank model has to be created. A cuboid of size $LXBXH$ where L , B and H are the length, breadth and height represents the geometry of the blank (Fig. 3). It has six planes bounding the block I-VI. The blank when machined on one end at arbitrarily chosen angles gives the sculptured cutting surfaces and edges making the form-cutting tool (Fig. 4). These free-form machined surfaces are represented through a CAD model.

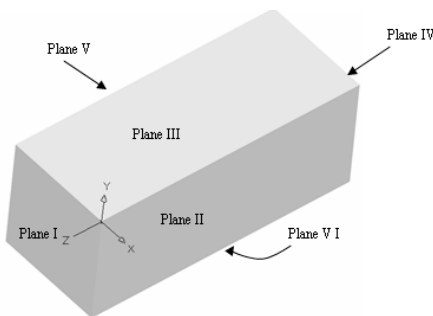


Fig. 3: System of planes for tool modeling.

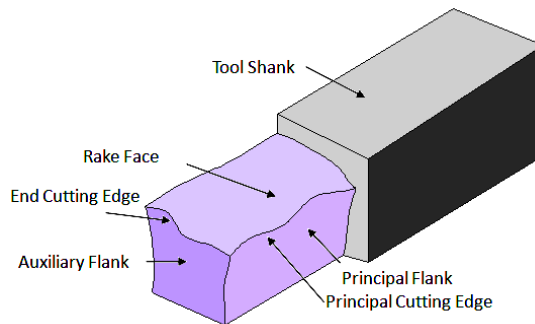


Fig. 4: Form-cutting tool machined from blank.

The face and flanks of the tool are modeled using surface patches represented parametrically using NURBS. When the weights assigned to the control points are unity, the representation is same as that of B-spline surfaces. A NURBS surface is represented by

$$\bar{c}(u,v) = \frac{\sum_{i=0}^n \sum_{j=0}^m w_{ij} N_{p,p+i}(u) N_{q,q+j}(v) \bar{c}_{ij}}{\sum_{i=0}^n \sum_{j=0}^m w_{ij} N_{p,p+i}(u) N_{q,q+j}(v)} \tag{3.1}$$

where, \bar{c}_{ij} represents the array of control points, p and q are orders of B-spline curves along the u - and v - directions respectively. The control points may be chosen selectively to represent the surfaces.

Now, let the surfaces on the cutting end of the tool be represented by

Auxiliary flank:
$$\bar{c}_a(u_1, v_1) = \frac{\sum_{i=0}^{n_a} \sum_{j=0}^{m_a} w_{ij}^a N_{p_a, p_a+i}(u_1) N_{q_a, q_a+j}(v_1) \bar{c}_{ij}^a}{\sum_{i=0}^{n_a} \sum_{j=0}^{m_a} w_{ij}^a N_{p_a, p_a+i}(u_1) N_{q_a, q_a+j}(v_1)} \quad (3.2)$$

Principal flank:
$$\bar{c}_f(u_2, v_2) = \frac{\sum_{i=0}^{n_f} \sum_{j=0}^{m_f} w_{ij}^f N_{p_f, p_f+i}(u_2) N_{q_f, q_f+j}(v_2) \bar{c}_{ij}^f}{\sum_{i=0}^{n_f} \sum_{j=0}^{m_f} w_{ij}^f N_{p_f, p_f+i}(u_2) N_{q_f, q_f+j}(v_2)} \quad (3.3)$$

Rake face:
$$\bar{c}_r(w_3, u_3) = \frac{\sum_{i=0}^{n_r} \sum_{j=0}^{m_r} w_{ij}^r N_{p_r, p_r+i}(w_3) N_{q_r, q_r+j}(u_3) \bar{c}_{ij}^r}{\sum_{i=0}^{n_r} \sum_{j=0}^{m_r} w_{ij}^r N_{p_r, p_r+i}(w_3) N_{q_r, q_r+j}(u_3)} \quad (3.4)$$

At the tool tip, $\bar{c}_a(u_{10}, v_{10}) = \bar{c}_f(u_{20}, v_{20}) = \bar{c}_r(w_{30}, u_{30})$.

To model the nose, it is represented as a ruled oblique cone with one curved edge (directrix) and two straight lines (generators). In general, there is no need to choose curves for generators as it does not help in functionality. The directrix is modeled parametrically as a curve, the simplest example being an arc. The vertex of the cone is obtained on the curve of intersection of the principal flank and the auxiliary flank. A model of nose in the form of a ruled surface has been shown in Fig. 5.

The parametric definition of the nose goes as follows:

$$q_n(u, v) = p(u, 0)(1 - v) + P^* v \quad (3.5)$$

where $p(u, 0)$ is the equation of the circular arc of the nose.

The above formulation is to be used when the user is free to choose the control points. When the data points in place of the control points are available, the following method has to be employed.

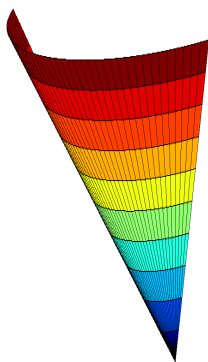


Fig. 5: Nose formation.

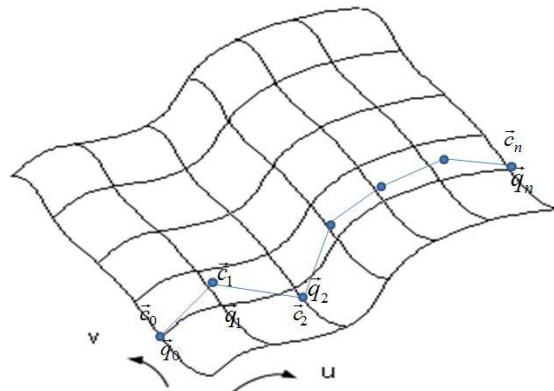


Fig. 6: Obtaining Control Points from data points.

3.1 Generating Control Points on the Surface

When the control points are not available but the points on the surface and cutting edge are given, the control points are to be extracted from the data points. This is generally the case when the points on the tool surface are extracted from an existing tool obtained through free-form grinding through some data capturing technique, be it contact or non-contact measurement. To obtain the control points, the data points are selected so that they form a rectangular matrix on the surface. Thus we have an array of curves passing through the given data points along the two directions, say the u - and v -direction shown in Fig. 6. Choosing u -direction, let the data points on any curve be $\bar{q}_0, \bar{q}_1, \dots, \bar{q}_n$. To fit them with a B-spline curve of order $p \leq n$, we select a set of parameters s_0, s_1, \dots, s_n corresponding to each data point. If the unknown control points are represented by $\bar{c}_i, i = 0 \dots n$, we have

$$\bar{c}(u) = \sum_{i=0}^n N_{p,p+i}(u) \bar{c}_i \quad (3.6)$$

Using the mapping of the data points and the parameters, we have,

$$\bar{q}_k = \bar{c}(s_k) = \sum_{i=0}^n N_{p,p+i}(s_k) \bar{c}_i, \quad k = 0 \dots n$$

$$\text{or, } \{Q\} = \begin{bmatrix} \bar{q}_0 \\ \bar{q}_1 \\ \dots \\ \dots \\ \bar{q}_n \end{bmatrix} = \begin{bmatrix} N_{p,p}(s_0) & N_{p,p+1}(s_0) & N_{p,p+2}(s_0) & \dots & N_{p,p+n}(s_0) \\ N_{p,p}(s_1) & N_{p,p+1}(s_1) & N_{p,p+2}(s_1) & \dots & N_{p,p+n}(s_1) \\ \dots & \dots & \dots & \dots & \dots \\ \dots & \dots & \dots & \dots & \dots \\ N_{p,p}(s_n) & N_{p,p+1}(s_n) & N_{p,p+2}(s_n) & \dots & N_{p,p+n}(s_n) \end{bmatrix} \begin{bmatrix} \bar{c}_0 \\ \bar{c}_1 \\ \dots \\ \dots \\ \bar{c}_n \end{bmatrix} = [N]\{C\} \quad (3.7)$$

$$\text{or, } \{C\} = [N]^{-1}\{Q\} \quad (3.8)$$

As the interpolating curve is spatial, each data point will have 3 cartesian coordinates (x_s, y_s, z_s) and same with the control points. Having obtained the control points, weights are assigned to each control point to give local shape control to the user. This converts the B-spline to NURBS giving freedom to modify the surface without changing the control points at a later stage if needed. This is required when the user wants a desired variation of rake or flank angles on the tool.

3.2 Cutting Edge Elements

As stated earlier, if the geometry of the sculptured work surface is known, the cutting edge of the tool can be derived based on the fulfillment of prescribed conditions. In case, the user wants to start with the definition of face and flank surfaces and derive the equation to the cutting edge subsequently, it becomes a surface-surface intersection problem, where the two surfaces have NURBS representation. To obtain the points of intersection of the intersecting 3D rake and flank surfaces, Timmer's algorithm for surface-surface intersection may be employed. Alternatively, it can be simplified as a surface-curve intersection problem too and the points of intersection obtained.

Another method to obtain the cutting edges is to use the optimization methods. The problem of intersection is formulated as an optimization problem as given below:

$$\min\{(\bar{d}|_{w_3})_x^2 + (\bar{d}|_{w_3})_y^2 + (\bar{d}|_{w_3})_z^2\}$$

The points of intersection are given by the points at which

$$(\bar{d}|_{w_3})_x^2 + (\bar{d}|_{w_3})_y^2 + (\bar{d}|_{w_3})_z^2 = 0 \quad (3.9)$$

where, $\bar{d}|_{w_3}$ gives the distance between the flank surface and a curve along the rake face for a chosen value of w_3

The intersection of $\bar{c}_f(u_2, v_2)$ and $\bar{c}_r(w_3, u_3)$ gives the principal (or side) cutting edge, while the intersection of $\bar{c}_a(u_1, v_1)$ and $\bar{c}_r(w_3, u_3)$ gives the end cutting edge.

After obtaining the points on the principal cutting edge, the edge is constructed as made up of small cutting elements. Let it be made up of elements represented by $\Delta\bar{l}$.

$$\Delta\bar{l} = \Delta l_x \hat{i} + \Delta l_y \hat{j} + \Delta l_z \hat{k} \quad (3.10)$$

where $\Delta l_x, \Delta l_y, \Delta l_z$ can be positive or negative. While calculating the tool angles, Δl_x has been taken as positive while Δl_y and Δl_z have been taken as negative. This is the case when the inclination angle is positive and principal cutting edge angle is acute. The formulation can be suitably adopted for different signs of the element components.

$$\text{For the } i^{\text{th}} \text{ element, let } \Delta\bar{l}_i = \Delta l_{ix} \hat{i} + \Delta l_{iy} \hat{j} + \Delta l_{iz} \hat{k} \quad (3.11)$$

$$\text{Similarly for the end cutting edge, let it be represented as } \Delta\bar{l}_e = \Delta l_{ex} \hat{i} + \Delta l_{ey} \hat{j} + \Delta l_{ez} \hat{k} \quad (3.12)$$

4 CUTTING ANGLES ON THE TOOL RAKE AND FLANKS

The normal to the auxiliary flank along the end cutting edge is $\bar{n}_a(u_1, v_1)$, to the principal flank along the principal cutting edge is $\bar{n}_f(u_2, v_2)$ and the normal to the rake face along the principal and end cutting edges are $\bar{n}_{rp}(w_3, u_3)$ and $\bar{n}_{ra}(w_3, u_3)$ respectively, where,

$$\bar{n}_a(u_1, v_1) = \bar{c}_{a,u_1}(u_1, v_1) \times \bar{c}_{a,v_1}(u_1, v_1) \quad (4.1)$$

and so on. Here $\bar{c}_{a,u_1}(u_1, v_1)$ and $\bar{c}_{a,v_1}(u_1, v_1)$ denote the tangents to the auxiliary flank in the u_1 - and v_1 - directions respectively along the cutting edge.

Using the projections of the normal vectors along the chosen planes, the ASA, ORS and NRS angles are calculated. It is clear that the angles will have different values for the different elements along the cutting edges. But for simplicity, the subscript i has been dropped while denoting the angles.

4.1 ASA Angles

The normal vectors to the rake face on the principal and end cutting edges are given respectively by:

$$\bar{n}_{rp} = n_{rpx} \hat{i} + n_{rpy} \hat{j} + n_{rpz} \hat{k} \quad (4.2)$$

$$\bar{n}_{re} = n_{rex} \hat{i} + n_{rey} \hat{j} + n_{rez} \hat{k} \quad (4.3)$$

Back and Side Rake Angles

When the normal \bar{n}_{rp} is projected on the YZ -plane, the dot product of the unit projected normal with unit vector \hat{j} gives the back rake angle γ_z . When it is projected on the XY -plane, it makes side rake angle γ_x with the Y -axis.

$$\text{Thus } \gamma_z = \cos^{-1} \left(\frac{n_{rpy}}{\sqrt{n_{rpy}^2 + n_{rpx}^2}} \right) \quad (4.4)$$

$$\text{and, } \gamma_x = \cos^{-1} \left(\frac{n_{rpy}}{\sqrt{n_{rpx}^2 + n_{rpy}^2}} \right) \quad (4.5)$$

The normal vector to the principal flank is given by

$$\vec{n}_f = n_{fx} \hat{i} + n_{fy} \hat{j} + n_{fz} \hat{k} \quad (4.6)$$

Clearance Angles

The clearance angle α_z is obtained as the angle between the projection of \vec{n}_f on the YZ-plane and the Z-axis. To obtain another clearance angle α_x , \vec{n}_f is projected on the XY-plane and the dot product of the unit normal projected vector with the X-axis gives α_x .

$$\text{Hence, } \alpha_z = \cos^{-1} \left(\frac{n_{fz}}{\sqrt{n_{fy}^2 + n_{fz}^2}} \right) \quad (4.7)$$

$$\text{and, } \alpha_x = \cos^{-1} \left(\frac{n_{fx}}{\sqrt{n_{fx}^2 + n_{fy}^2}} \right) \quad (4.8)$$

Similarly, the clearance angles on the auxiliary flank are to be obtained.

Side and End Cutting Edge Angles

For the designed single point cutting tool, for each element on the side (principal) cutting edge, the projection of the element on the base plane ($\Delta \vec{l}_3 = \Delta l_x \hat{i} + \Delta l_z \hat{k}$) is evaluated.

The angle made by $\Delta \vec{l}_3$ with the Z-axis gives the side cutting edge angle ϕ_s .

$$\text{Thus } \phi_s = \tan^{-1} \left(\frac{|\Delta l_x|}{|\Delta l_z|} \right) \quad (4.9)$$

Similarly the angle made by the elements of the projection of the end cutting edge on the base plane with the X-axis gives the end cutting edge angle ϕ_e . It is obtained as given below:

$$\text{Projected on the base plane, it gives } \Delta \vec{l}_{e3} = \Delta l_{ex} \hat{i} + \Delta l_{ez} \hat{k} \quad (4.10)$$

$$\text{The end cutting edge angle is given as } \phi_e = \tan^{-1} \left(\frac{|\Delta l_{ez}|}{|\Delta l_{ex}|} \right) \quad (4.11)$$

Of course, the angles will vary for every element.

4.2 ORS Angles

Principal and End Cutting Edge Angles

The principal cutting edge angle ϕ is the angle made by the projection of the principal cutting edge on the base plane with the X-axis. It is the compliment of the side cutting edge angle.

$$\text{Thus } \phi = \frac{\pi}{2} - \phi_s \quad (4.12)$$

The end cutting edge angle remains the same.

Orthogonal Rake Angle (γ_o) and Inclination Angle (λ)

To obtain γ_o , \vec{n}_{rp} is rotated by an angle $(90^\circ - \phi)$ ccw about the Y-axis which is given as \vec{n}_{rr} and projected on the XY-plane. The dot product of the unit normal projected vector with the Y-gives γ_o .

$$\text{Thus } \gamma_o = \cos^{-1} \left(\frac{n_{rpy}}{\sqrt{(n_{rpx} \sin \phi + n_{rpz} \cos \phi)^2 + n_{rpy}^2}} \right) \quad (4.12)$$

λ is obtained as the angle between the projection of the vector \vec{n}_{rr} on the YZ-plane and the Y-axis. Thus,

$$\lambda = \cos^{-1} \left(\frac{n_{rpy}}{\sqrt{(-n_{rpx} \cos \phi + n_{rpz} \sin \phi)^2 + n_{rpy}^2}} \right) \quad (4.13)$$

Orthogonal Clearance Angles α_o and α_o'

The clearance angles are obtained in a similar manner as the rake angle. \vec{n}_f is rotated about the Y-axis ccw by $(90^\circ - \phi)$ and projected on the XY- plane. The dot product of the unit normal projected vector \vec{n}_{pr1} with the X-axis gives α_o .

To obtain the orthogonal clearance angle on the auxiliary flank α_o' , \vec{n}_a is rotated about the Y-axis ccw by ϕ_e and projected on the XY- plane. The dot product of this unit normal projected vector \vec{n}_{ar1} with the X-axis gives α_o' .

4.3 NRS Angles

The angles ϕ , ϕ_e , λ and will have the same values.

To obtain the normal rake angle, the following relations can be used:

$$\gamma_n = \tan^{-1} [\tan \gamma_o \cos \lambda] \quad (4.14)$$

$$\alpha_n = \tan^{-1} \left[\frac{\tan \alpha_o}{\cos \lambda} \right] \quad (4.15)$$

$$\alpha_n' = \tan^{-1} \left[\frac{\tan \alpha_o'}{\cos \lambda} \right] \quad (4.16)$$

5 MECHANISTIC FORCE MODELING

The values of the tool angles obtained in ASA, ORS and NRS systems can now be fitted in the mechanistic equation to get the specific cutting pressures. A mechanistic equation has the general form

$$\begin{aligned} F_n &= K_n \cdot A_c \\ F_f &= K_f \cdot A_c \end{aligned} \quad (5.1)$$

where K_n is the specific normal pressure, K_f is the specific friction pressure and A_c is given by:

$A_c = t_c \cdot w$ (t_c is the uncut chip thickness and w is the depth of cut). The specific normal pressure and friction pressure depend on the tool workpiece material combination, the cutting conditions and the cutting geometry, and are determined by fitting experimental data in a process called calibration.

For HSS tool and MS material combination, where the composition of MS is given as 0.24 %C, 0.67% Mn, 0.16% Si, 0.027%S, 0.035%P with 128 BHN Hardness, a mechanistic equation was generated by Sambhav et al. [15] in terms of the ASA, ORS and NRS nomenclature is given below.

In terms of ASA angles, the equation is presented as:

$$K_n = +7663.68 - 224.00\gamma_x + 95.14\phi_s - 48.07V - 22263.62f + 1.07\gamma_x \cdot V + 471.71\gamma_x \cdot f - 2.34\phi_s \cdot V + 266.50V \cdot f \quad (5.2)$$

$$K_f = +6537.58 - 118.62\gamma_x + 53.75\phi_s - 34.01V - 22382.26f + 1.21\gamma_x.V + 269.07\gamma_x.f - 1.41\phi_s.V + 227.53V.f \quad (5.3)$$

In terms of ORS angles, it is presented as:

$$K_n = +16226.64 - 226.14\gamma_o - 95.14\phi - 258.92V - 22263.62f + 1.09\gamma_o.V + 478.48\gamma_o.f + 2.34\phi.V + 266.50V.f \quad (5.4)$$

$$K_f = +11374.98 - 119.60\gamma_o - 53.75\phi - 160.64V - 22382.26f + 1.23\gamma_o.V + 272.18\gamma_o.f + 1.41\phi.V + 227.53V.f \quad (5.5)$$

In terms of NRS angles, it is presented as:

$$K_n = +16226.64 - 227.73\gamma_n - 95.14\phi - 258.92V - 22263.62f + 1.10\gamma_n.V + 482.07\gamma_n.f + 2.34\phi.V + 266.50V.f \quad (5.6)$$

$$K_f = +11374.98 - 120.44\gamma_n - 53.75\phi - 160.64V - 22382.26f + 1.24\gamma_n.V + 274.18\gamma_n.f + 1.41\phi.V + 227.53V.f \quad (5.7)$$

For the above equation, the range for variation for the parameters is shown in Tab. 1.

S. No.	Unit	Parameter	Low	High
1	Degree	Rake angle	-20	20
2	Degree	Principal cutting edge angle	80	110
3	m/min	Velocity	16.33	65.34
4	mm/rev	Feed	0.05	0.175

Tab. 1: Range of variation of parameters.

For any free-form SPCT, the above equation can be applied and the normal and friction forces obtained. Assuming Stabler's Rule to hold true, the force transformation relation are given as:-

$$\begin{Bmatrix} F_c \\ F_t \\ F_l \end{Bmatrix} = \begin{bmatrix} c\lambda.c\gamma_n & s^2\lambda + c^2\lambda.s\gamma_n \\ -s\gamma_n & c\lambda.c\gamma_n \\ s\lambda.c\gamma_n & c\lambda.s\lambda.s\gamma_n - s\eta_c.c\lambda \end{bmatrix} \begin{Bmatrix} F_n \\ F_f \end{Bmatrix} \quad (5.8)$$

Where F_c is the cutting force, F_t is the thrust force and F_l is the lateral force. Thus the cutting and thrust forces can be obtained for different experimental conditions.

6 EXPERIMENTAL WORK

An HSS tool was arbitrarily ground and a free-form geometry generated on the tool (Fig. 7). It was mounted on a micro-machining center installed in the manufacturing science lab at IIT Kanpur. The regions of the cutting tool which had to be used for turning were marked and data points on the cutting edge in the chosen regions were obtained. To obtain the rake face, two curves on the rake face, one along the cutting edge and one adjoining the cutting edge were chosen and 10 data points were captured on each curve on an Integrated Multi-process Machine Tool DT-110 by Mikrotools with a 300 micron probe. Using Eq (3.8), the control points were obtained and the two curves were fitted with B-splines. The normal rake angle and principal cutting edge angle were obtained along the cutting edge. As only two curves were required to get the tool angles on the cutting edge, B-spline curve fitting in the transverse direction was not required. A random value of feeds and speeds to be used for turning were selected and the theoretical values of cutting and thrust forces were obtained mechanistically using Eqn. (5.6) and Eqn. (5.7). The feeds and speeds used for the experiment are given in Tab. 2.

An MS tubular workpiece of mean diameter 26 mm with the composition mentioned above was selected and turned to the desired thickness of 3 mm. Then the workpiece was turned at the chosen

feeds and speeds using the selected regions of the cutting tool. Two such regions on the arbitrarily ground HSS tool were used, one with a convex profile and the other with a concave profile (Fig. 8). The forces were recorded on a 3-Component Quartz Dynamometer of 9257BA model with 3-channel built-in charge amplifiers and 4 switchable measuring ranges and compared with the analytically obtained values.



Fig. 7: SPCT with free-form cutting edge.

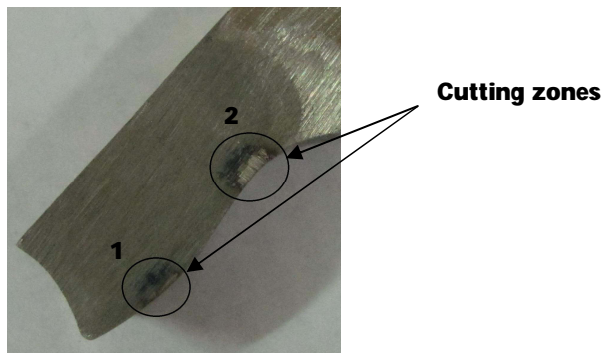


Fig. 8: Cutting zones on the cutting edge.

S. No.	RPM	Feed (mm/rev)
1	320	0.088
2	320	0.113
3	640	0.088
4	640	0.113

Tab. 2: Speed and Feed used for the experiment.

7 RESULTS AND DISCUSSION

The experimental and theoretical results for the two zones of the cutting tool are shown in Tabs. 3 and 4. Zone 1 had a higher rake angle and a lower principal cutting edge angle on an average as compared to zone 2. The comparison of the two values shows a good correlation and establishes the usefulness of the force model. The maximum error observed is 8.27% when calculated with respect to the experimental values. The possible sources of error are the uncertainty involved in the capturing of data from the tool and the wearing of the tool surface which changes the profile.

S.No.	Speed (m/min)	Feed (mm/rev)	Cutting Force (Newtons)			Thrust Force (Newtons)		
			Theoretical	Experimental	Error	Theoretical	Experimental	Error
1	27.14	0.088	985.3	923.5	6.69%	621.3	596.3	4.19%
2	27.14	0.113	1210.1	1185.3	2.09%	814.8	787.9	3.41%
3	54.28	0.088	674.9	685.5	-.54%	611.8	567.8	7.75%
4	54.28	0.113	869.9	886.1	-.83%	784.6	780.3	0.55%

Tab. 3: Comparison of cutting and thrust forces for zone 1.

S.No.	Speed (m/min)	Feed (mm/rev)	Cutting Force			Thrust Force		
			Theoretical	Experimental	Error	Theoretical	Experimental	Error
1	27.14	0.088	1124.6	1158.8	- 2.95%	812.2	756.4	7.38%
2	27.14	0.113	1351.2	1415.5	- 4.54%	1056.2	1023.1	3.23%
3	54.28	0.088	1026.7	948.3	8.27%	806.9	749.7	7.63%
4	54.28	0.113	1285.6	1239.3	3.74%	1040.8	1018.3	2.21%

Tab. 4: Comparison of cutting and thrust forces for zone 2.

8 SUMMARY AND CONCLUSIONS

The presented work is an attempt to geometrically model a form-cutting tool using CAD and apply the mechanistic methods to predict the forces during cutting. Such a formulation is highly useful for predicting the forces, tool life, wear pattern and tool failure for form tools. The accomplished work can be summed up as follows:

- The geometry of single point cutting tool with free-form rake and flank surfaces are modeled using NURBS.
- The rake and flank angles are evaluated for different nomenclatures at different points of the cutting edge using projections of the normal to the surfaces along different planes.
- The mechanistic equations [15] for specific normal and friction forces in terms of rake angle, principal cutting edge angle, speed and feed are employed to find out the cutting and thrust forces.
- To evaluate the CAD model coupled with the mechanistic equation, an HSS tool was arbitrarily ground and used for cutting an MS workpiece. The theoretical and experimental values were compared, and the comparison showed a good correlation between the results.

Based on the work proposed in the paper, it is concluded that CAD can be effectively used for the geometric design of form-cutting tools. Using semi-empirical methods such as mechanistic model, the CAD model can be used to predict the forces in cutting. The present work uses turning for evaluation of model but as the mechanistic model is specific to a particular tool-workpiece combination only, and not any machining process, the same formulation can be applied for other machining processes too. Thus coupling CAD with mechanistic methods shows a good prospect for design of form-cutting tools.

References

- [1] Karunakaran, K. P.: Geometric Modeling of Manufacturing Processes using Symbolic and Computational Conjugate Geometry, Ph.D. Thesis, IIT Kanpur, 1993.
- [2] Radzevich, S. P.: R-Mapping Based Method of Designing of Form Cutting Tool for Sculptured Surface Machining, *Mathematical and Computer Modeling*, 36, 2002, 921-938. [http://dx.doi.org/10.1016/S0895-7177\(02\)00237-6](http://dx.doi.org/10.1016/S0895-7177(02)00237-6)
- [3] Radzevich, S. P.: Conditions of Proper Sculptured Surface Machining, *Computer Aided Design*, 34, 2002, 727-740. [http://dx.doi.org/10.1016/S0010-4485\(01\)00202-0](http://dx.doi.org/10.1016/S0010-4485(01)00202-0)
- [4] Radzevich, S. P.: A novel method for mathematical modeling of a form-cutting-tool of the optimum design, *Applied Mathematical Modeling*, 31, 2007, 2639-2654. <http://dx.doi.org/10.1016/j.apm.2006.10.014>

- [5] Fan, J.; Ball, A.: Quadric method for cutter orientation in 5-axis sculptured surface machining, *International Journal of Machine Tools & Manufacture*, 48, 2008, 788-801. <http://dx.doi.org/10.1016/j.ijmachtools.2007.12.004>
- [6] Li, S. X.; Jerard, R. B.: 5-axis machining of sculptured surfaces with a flat-end cutter, *Computer Aided Design*, 26(3), 1994, 165-178. [http://dx.doi.org/10.1016/0010-4485\(94\)90040-X](http://dx.doi.org/10.1016/0010-4485(94)90040-X)
- [7] Lee, Y. S.: Non-isoparametric tool path planning by machining strip evaluation for 5-axis sculptured surface machining, *Computer Aided Design*, 30(7), 1998, 559-570. [http://dx.doi.org/10.1016/S0010-4485\(98\)00822-7](http://dx.doi.org/10.1016/S0010-4485(98)00822-7)
- [8] Fussel, B. K.; Jerard, R. B.; Hemmet, J. G.: Modeling of Cutting Geometry and Forces for 5-axis sculptured surface machining, *Computer Aided Design*, 35, 2003, 333-346. [http://dx.doi.org/10.1016/S0010-4485\(02\)00055-6](http://dx.doi.org/10.1016/S0010-4485(02)00055-6)
- [9] Liu, X. W.: Five-axis NC cylindrical milling of sculptured surfaces, *Computer Aided Design*, 27(12), 1995, 887-894. [http://dx.doi.org/10.1016/0010-4485\(95\)00005-4](http://dx.doi.org/10.1016/0010-4485(95)00005-4)
- [10] Park, S. C.: Sculptured surface machining using triangular mesh slicing, *Computer-Aided Design*, 36, 2004, 279-288. [http://dx.doi.org/10.1016/S0010-4485\(03\)00114-3](http://dx.doi.org/10.1016/S0010-4485(03)00114-3)
- [11] Zhongqing, W.: Research on forming theory of a 3D body by the cutting geometry method (CCG) *Journal of Materials Processing Technology*, 139, 2003, 539-542. [http://dx.doi.org/10.1016/S0924-0136\(03\)00521-1](http://dx.doi.org/10.1016/S0924-0136(03)00521-1)
- [12] Sambhav, K.; Tandon, P.; Dhande, S. G.: A generic mathematical model of single point cutting tool in terms of grinding angles, *Applied Mathematical Modeling*, 35(10), 2011, 5143-5164. <http://dx.doi.org/10.1016/j.apm.2011.04.017>
- [13] Lamikiz, A.; Lacalle, L. N. L.; Sanchez, J. A.; Salgado, M.A.: Cutting force estimation in sculptured surface milling, *International Journal of Machine Tools & Manufacture*, 44, 2004, 1511-1526. <http://dx.doi.org/10.1016/j.ijmachtools.2004.05.004>
- [14] Lazoglu, I.: Sculpture surface machining: a generalized model of ball-end milling force system, *International Journal of Machine Tools and Manufacture*, 43, 2003, 453-462. [http://dx.doi.org/10.1016/S0890-6955\(02\)00302-4](http://dx.doi.org/10.1016/S0890-6955(02)00302-4)
- [15] Sambhav, K.; Tandon, P.; Dhande, S.G.: Mechanistic force modeling of single point cutting tool in terms of grinding angles, *International Journal of Machine Tools & Manufacture*, 51, 2011, 775-786. <http://dx.doi.org/10.1016/j.ijmachtools.2011.06.007>